Available online at www.sciencedirect.com
ScienceDirect
Journal of Molecular Graphics and Modelling 25 (2006) 396–409
Journal of Molecular Graphics and Modelling
www.elsevier.com/locate/JMGM

Molecular dynamics of a biophysical model for β_2-adrenergic and G protein-coupled receptor activation☆

Lester A. Rubenstein [a,✠], Randy J. Zauhar [b], Richard G. Lanzara [c,*]

[a] *Department of Physiology and Biophysics, Mount Sinai School of Medicine, One Gustav Levy Place, New York, NY 10029, United States*
[b] *Department of Chemistry and Biochemistry, The University of the Sciences in Philadelphia, 600 S. 43rd Street, Philadelphia, PA 19104, United States*
[c] *Bio Balance, Inc. Pharmacology, 30 West 86th Street, New York, NY 10024, United States*

Received 14 December 2005; received in revised form 17 February 2006; accepted 21 February 2006
Available online 30 March 2006

Abstract

This study analyzes 16 molecular dynamic simulations of a biophysical model for β_2-adrenergic (B2AR) and G protein-coupled receptor (GPCR) activation. In this model, a highly conserved cysteine residue, C106 (C3.25 or CysIII:01), provides a free sulfhydryl or thiol group in an acid–base equilibrium between uncharged (RSH) and charged (RS^-) states that functions as an electrostatic molecular switch for receptor activation. The transition of C106 in the B2AR between acid and base states significantly changes the helical/transmembrane (TM) domain interactions and the electrostatic interaction energy differences ($\Delta\Delta E^{EL}$). The $\Delta\Delta E^{EL}$ changes correlate well with the experimentally observed ligand efficacies. The TM interaction energies display patterns compatible with those previously recognized as responsible for GPCR activation. Key differences between the agonist, epinephrine, and the antagonist, pindolol, are seen for the TM3 × 6, TM3 × 4, TM6 × 7 and TM1 × 7 interaction energies. Pindolol also produces a weaker $\Delta\Delta E^{EL}$ interaction and less TM interaction energy changes, which are important differences between the agonist and antagonist ligands. The D115E mutant with pindolol displays a greater $\Delta\Delta E^{EL}$ and TM interactions than for the wild-type B2AR with pindolol. This explains the higher activity of pindolol in the D115E mutant. The constitutively active D130A mutant displays TM interaction patterns similar to those for the activating ligands implying a common pattern for receptor activation. These findings support the broad concept of protean agonism and demonstrate the potential for allosteric modulation. They also demonstrate that this two-state model agrees with many previous experimental and theoretical observations of GPCRs.

Keywords: Molecular dynamics; Two-state model; G protein-coupled receptor model; B2AR adrenergic receptor; Sulfhydryl; Electrostatic molecular switch; Receptor activation

1. Introduction

Receptor activation requires the recognition of an extracellular signal that usually involves an endogenous agonist ligand activating its target receptor. The G protein-coupled receptors (GPCRs), receive and transmit these signals to the intracellular environment. As general models for all GPCRs, the β_2-adrenergic (B2AR) and rhodopsin receptors have been studied extensively to understand the complex molecular changes that accompany receptor activation and signal transduction.

Recent experimental discoveries have significantly changed our understanding of how these receptors work. Bond et al. demonstrated that transgenic mice with an increased number of

Abbreviations: B2AR, β_2-adrenergic receptor; DTT, dithiolthreitol; D130A, the B2AR aspartate residue 130 to alanine mutation; D113E, the B2AR aspartate residue 113 to glutamate mutation; EPI, epinephrine; ΔEL, the energy difference between the base and acid states for the electrostatic energy terms; $\Delta\Delta E^{EL}$, electrostatic interaction energy differences; GPCR, G protein-coupled receptor; G_s, stimulatory GTP-binding regulatory protein of adenylylcyclase; ΔLJ, the energy difference between the base and acid states for the Lennard–Jones energy terms; MD, molecular dynamics; NE, norepinephrine; PIN, pindolol; RMSD, root mean square deviation; ΔRH, the net change in a high affinity receptor state; TM, transmembrane

☆ This work is dedicated to and in memory of Dr. Lester A. Rubenstein.

* Corresponding author.
E-mail address: rlanzara@bio-balance.com (R.G. Lanzara).
✠ Deceased author.

1093-3263/$ – see front matter © 2006 Elsevier Inc. All rights reserved.
doi:10.1016/j.jmgm.2006.02.008

B2AR receptors exhibit spontaneous activity similar to normally expressed receptors in the presence of an agonist ligand [1]. This observation separated receptor activation from the action of agonist ligands alone and prompted a revision of receptor models to include an intrinsically active receptor state. One consequence of this revision was that the resting populations of receptors must interconvert *by themselves* from resting to active states. However, the biophysical basis for these active and inactive receptor states has not been adequately defined or understood. One possible perspective is that there must exist an equilibrium between the inactive and active receptor states that can be perturbed to produce a shift in the net amounts of these states. An agonist ligand favoring the active receptor state would perturb the initial chemical equilibrium thereby inducing receptor activation in a manner similar to Le Chatelier's principle. However, the underlying molecular mechanism of this perturbation needs to be more carefully examined.

Mathematical models are essential for understanding the underlying biophysical events that determine the receptor response. In general, two-state mathematical models have been among the most successful for describing receptor activation [2–8]. Most of these models calculate either the proportional or fractional receptor occupancy as the overall receptor response [2–5]. Although it is seductive to assume that the proportional amount of an active receptor state should correlate with the biological response, the experimental evidence for receptor overexpression and spare receptors suggests that the calculation of the *net* change in the active receptor state is a much better measure for response than is the fractional or proportional change [6–8]. This is demonstrated by the effects of agonist/antagonist combinations on the desensitization of β-receptors [7,8]. This is also demonstrated by receptors that are activated by overexpression since this requires a change between R and R^* that is difficult to understand in terms of a proportional rather than a net change [7,8]. From this perspective, it is important to determine within the constructs of any molecular model what molecular states interconvert either by ligands, receptor overexpression or mutation.

Several experimental techniques show that the relative movements of transmembrane domains III and VI (TM3 and TM6) correspond with receptor activation in both the rhodopsin and B2AR receptors [9–15]. Gether et al., using fluorescent labels, localized agonist-induced conformational changes of the B2AR to TM3 and TM6 [12]. Ballesteros et al. showed that charge-neutralizing mutations of E268 in TM6 and D130 in TM3 led to a significant increase in basal and pindolol-stimulated cAMP accumulation in COS-7 cells, which was presumably due to an increase in the relative motions of TM3 to TM6 [13,14]. In the rhodopsin receptor, Khorana's group using spin labels attached to cysteine residues showed that rigid body movements of TM3 relative to TM6 were essential for activation [10].

Other investigators have also suggested that the *cis–trans* isomerization of retinal in rhodopsin causes repositioning followed by a movement of TM3 away from TM6 [9,11,15]. Clearly there are many studies that implicate TM3 and TM6 with the molecular events leading to receptor activation. An implicit assumption from these important studies is that there exists an ''off'' conformation of the TM3 and TM6 domains that can be switched to an ''on'' conformation corresponding with GPCR activation. However, from this perspective, it is difficult to clearly translate TM3 and TM6 domain motions into discrete molecular entities for specific on and off states. Previously, we have attempted to bridge this gap by defining specific receptor states that relate the acid–base transition of a conserved sulfhydryl group to the mathematically defined R and R^* states [16]. In this present work, we examine whether or not this model can be applied to the molecular dynamic analysis of the B2AR.

Although controversial, there is a wealth of experimental evidence for the existence of at least one free sulfhydryl group that modulates the receptor response in many GPCRs [16–34]. For decades it has been known that there are free sulfhydryl groups in blood and on the external side of animal tissues in vivo [17]. However, most experimentalists and theoreticians have not seriously questioned that the conserved disulfide-bonded cysteines may be a potential source of free sulfhydryl groups under normal physiologic conditions. This may be primarily due to the fact that all of the GPCR families are considered to have a highly conserved disulfide bond connecting a conserved cysteine in the extracellular region of TM3 [19–21]. Within all of the GPCR families this disulfide-linked cysteine, C110 in rhodopsin or C106 in the B2AR, is the most conserved cysteine that is vital for GPCR expression and function [19–21]. This disulfide's proximity to both the extracellular region and the ligand binding region suggests that the oxidation/reduction state of this bond could modulate both ligand binding and receptor function [23–25].

From specific sequence analyses, it is known that the B2AR receptor contains a total of 13 cysteine residues [18]. Of these cysteines, there are four potentially reactive cysteines, C106, C184, C190 and C191, on the external side of the B2AR that may form at least one extracellular disulfide bond [18]. Similarly, in the rhodopsin receptor there are three external cysteines, C110, C185 and C187 that are potentially reactive. The odd number of external cysteines in the rhodopsin receptor insures that there will be at least one free sulfhydryl group even when the disulfide bond is formed.

The crystal structure for rhodopsin in the Protein Data Bank (1F88) shows C110 in the extracellular region of TM3 positioned about 10 Å away from the 11-*cis*-retinal chromophore and 7 Å from glutamine E113 [15,22]. This C110 is normally considered to be in a disulfide bond with C187 and is apparently in a disulfide bond in the crystal structure; however, the nearby C185 apparently exists as a free sulfhydryl group, which may undergo acid–base transitions as well as other chemical reactions. Because the conditions for crystallization are very different from the natural state in which receptors normally function in vivo, it is difficult to imagine that the conditions for crystallization would preserve the free sulfhydryl groups of a reduced disulfide bond. Receptors transiently exposed to oxidizing conditions in vivo or in vitro may form this disulfide bond as a protective mechanism so that upon return to

reducing conditions, the normal receptor state could be easily regenerated.

In this context, it is important to consider a few of the complex chemical equilibria between the acid/base and oxidized/reduced forms of cysteine [35]. First, the side chain can reversibly ionize:

$$RSH \leftrightarrow RS^- + H^+ \quad (1)$$

Second, there is the oxidation/reduction equilibrium involving the disulfide bond:

$$RSH + RS^- \leftrightarrow RSSR + OH^- \quad (2)$$

In the presence of a suitable oxidizing agent, a suitable base acts to increase the probability of disulfide bond formation by forming RS^-, which initiates the reaction cascade for disulfide bond formation (shown below) [36].

In general, many sulfhydryl groups or mercaptans are easily oxidized to disulfides and the interconversion between cysteine and cystine is important in biochemistry [36]. This mechanism has been studied for several oxidizing agents and varies with the agent. For oxygen it is:

$$RSH + B^- \leftrightarrow RS^- + BH$$

$$RS^- + O_2 \leftrightarrow RS^{\bullet} + O_2^{\bullet -}$$

$$RS^- + O_2^{\bullet -} \leftrightarrow RS^{\bullet} + O_2^{2-}$$

$$2RS^{\bullet} \leftrightarrow RSSR$$

$$O_2^{2-} + BH \leftrightarrow OH^- + B^- + O_2$$

This mechanism with respect to the sulfur involves the loss of a proton, reduction to a free radical followed by radical coupling [36]. The resultant equation from this reaction cascade is Eq. (2) above. This reaction cascade demonstrates the important role played by base ions (B^-) to favor free radical formation in the presence of an oxidizing agent such as molecular oxygen. This also demonstrates some of the experimental difficulties in studying free thiol groups since exposure to air in the presence of a base is often sufficient to oxidize free thiols to disulfides or several other oxidized species too numerous to mention here [35–39].

From the above considerations, assumptions that the disulfide cysteines are always resistant to chemical derivatization may not be correct for the normal conditions of receptor function in vivo. When one or more of the extracellular cysteines of the B2AR (C106, C184, C190 or C191) are either mutated or chemically altered thiol/disulfide exchange may occur with the remaining free cysteines or other free thiol groups to complicate the analysis. In addition, double mutants often fail to express either as an extracellular or functional form of the receptor, which makes it difficult to determine which of the four cysteines in the B2AR are most critical for receptor function and expression [18,19]. This is usually interpreted as evidence for the disulfide bond being essential for receptor activation [18,19]. Although this view has been accepted without very much critical questioning, there is at least one alternative explanation [16].

Evidence from experimental binding studies from several GPCRs demonstrate that a free sulfhydryl group is next to the agonist ligand binding site [26–33]. Sidhu made use of this fact to purify the D-1 dopamine receptor from rat striatum [26]. Others using a morphine ligand with an attached sulfhydryl group found a free sulfhydryl group near the ligand binding site of the μ opioid receptor [27].

Additional studies have found free sulfhydryl groups next to the agonist binding site in the μ, δ and κ opioid receptors [28,29]. Heinonen et al., using a series of SH-reactive ''molecular yardsticks'', found a cysteine thiol group about 8.6–14.5 Å from the position of Asp113 (D113) in the α_2-adrenergic receptor [30]. Since this aspartate residue is important for attracting the positive amine group of binding ligands in many GPCRs including the B2AR, the proximity of free cysteines may be considered as a critical component of normal receptor function, which has been experimentally observed [23,24,31–34] and theoretically justified [16].

Experimental measurements of receptor activation suggest that the disulfide bond requires reduction to a free sulfhydryl for the functional state of several GPCRs in vivo [23–25,34]. One of the simplest and most direct experimental studies demonstrated that externally applied sulfhydryl reducing agents potentiate the response of tissues to various agonist ligands [34]. This study found that the reduction of disulfide bonds to free sulfhydryls increased the tissue responsiveness for many receptors and increased the potency of many agonists [34]. One problem with these studies is that physiologically opposing receptors may be simultaneously stimulated by the application of thiol reducing agents, which would confuse the analysis of the tissue response.

Additional evidence for the requirement of reduction for normal receptor function is evident in a number of other important studies. A free sulfhydryl group in the active rhodopsin receptor state is suggested from the MI to MII equilibrium shift of 4 units from a pK of 4.1 for ligand-free opsin to 8.5 [3]. This is also supported by the findings of Saranak and Foster that implicate a free sulfhydryl in the reductive activation of the rhodopsin photoreceptor [23]. For the muscarinic receptors, Florio and Sternweis found that the reducing agent DTT produced functional activation and potentiated agonist activation [25]. Pedersen and Ross using purified β-adrenergic receptors and purified G_s protein in phospholipid vesicles found that the treatment of these receptors with the sulfhydryl reducing agent dithiolthreitol (DTT) activated the G protein in either the presence or absence of agonist [24]. Since there was no effect of DTT on G_s alone, they reasoned that it was the receptor itself that was the target of the reducing agent and not the G protein [24]. Several other studies have also shown that constitutive activation occurred in reconstituted systems containing both β-adrenergic receptors and G proteins when the membrane vesicles were prepared with sulfhydryl reducing agents [31–33]. These experimental findings need to be included into a comprehensive model for receptor activation.

Previously, the acid and base states of the sulfhydryl group within the C148 residue in the 5-HT2A receptor were linked to

the inactive and active receptor states R and R^* [16]. In the current study, we have extended this model to the B2AR where the corresponding cysteine residue is C106 (C3.25 or CysIII:01). This cysteine, located on the extracellular side of TM3, functions as a molecular switch that toggles between the charged (RS^-) and uncharged (RSH) states associated with the acid to base transition of the sulfhydryl group [16]. This provides a specific molecular switch for receptor activation that correlates well with both the ligand induced electrostatic interaction energy difference ($\Delta\Delta E^{EL}$) and the experimentally measured ligand efficacies and the preferential attraction of ligands for the base receptor state (RS^-) [16]. In this context, ligand-induced perturbations produce a net change in the amount of the base receptor state (RS^-), that can mathematically describe the receptor response in a two-state model [6,7].

For this study, we examined 16 molecular dynamic (MD) simulations of full agonists, partial agonists and an antagonist of the wild-type and two mutant B2ARs. The D130A mutant changed the aspartate residue D130 in the DRY portion of TM3 to alanine. This mutation removes a negatively charged residue from the B2AR and produces a constitutively active receptor in at least two separate systems [14,40]. The other mutant is the D113E that replaces the aspartate residue D113 (D3.32) with a glutamate residue. This mutation does not alter the net charge of the receptor, but profoundly alters ligand efficacies causing both the antagonist pindolol and the full agonist norepinephrine to behave like partial agonists [19]. This behavior is examined through these simulations of B2AR activation within the context of this two-state acid–base model for GPCR activation.

2. Methodology

2.1. The molecular model

The B2AR model displayed in Fig. 1 was developed and further refined from the "What-IF" structures produced by Vriend at the EMBL labs in Heidelberg, which is based upon Baldwin et al.'s general model [20]. The D130A and D113E mutant structures were also modified from this B2AR model.

For this model, the change of the sulfhydryl group in C106 is associated with the acid and base states in the B2AR (see Fig. 1), which allows the sulfhydryl group to exist in either acid or base states (SH or S^-) [16]. Since the conserved Cys106 is located near the extracellular region, nearby water molecules would be expected to influence or modulate this electrostatic switch, but we did not model this possibility.

The receptor models comprising the seven transmembrane regions were constructed with the program QUANTA. The loop regions were not considered in this particular model although future work may require the inclusion of these elements. All hydrogen atoms were included explicitly. Standard CHARMM charges were applied to all receptor atoms except for the base state of the cysteine (C106 or C3.25) in which case the charges were derived from a calculation of the molecule ethyl sulfide with a 6–31G basis set using the Hartree–Fock method. The calculated charges were then scaled and adapted to CHARMM format. Ligand models in the form of cations were built with the

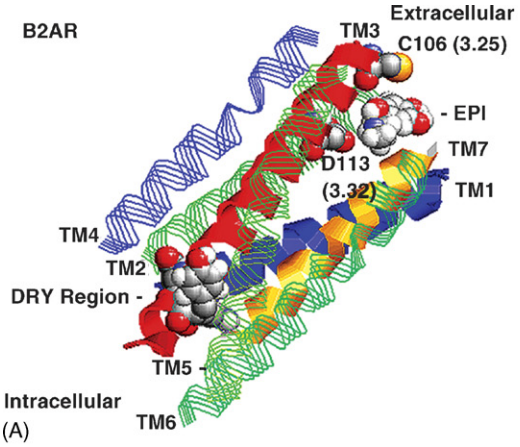

(A)

The B2AR Sequences:

TM1(EC to IC)§:
M G I V M S L I V L A I V F G N* V L V I T A I A

TM2(IC to EC):
V T N Y F I T S L A C A D* L V M G L A V V P F G

TM3(EC to IC):
106 113 130
W C† G F W T S I D V L C V T A S I E T L C V I A V D R* Y F A I T S

TM4(IC to EC):
K A R V I I L M V W* I V S G L T S F L P I Q M

TM5(EC to IC):
I A S S I V S F Y V P* L V I M V F V Y S R V F Q E A K R

TM6(IC to EC):
K E H K A L K T L G I I M G T F T L C W L P* F F I V N I

TM7(EC to IC):
I L L N W I G Y V N S G F N P* L I Y C R S P D

B2AR mutants of the TM3 residues:

D113E: (**D3.32** or **D113** to **E113**)
D130A: (**D3.49** or **D130** to **A130**)

§ **(EC to IC)** is the direction of this transmembrane domain from extracellular **(EC)** to intracellular **(IC)**. Because of the way sequences are written, the direction of the **EC** and **IC** ends alternate. Therefore TM1, TM3, TM5 and TM7 are **EC to IC** whereas TM2, TM4 and TM6 are **IC to EC.**

* Conserved residues in each TM domain 1.50, 2.50, 3.50, 4.50, 5.50, 6.50 and 7.50 (Ballesteros JA, Weinstein H, Methods Neurosci 1995; 25: 366-428).

† **C** (**C3.25** or **C106** - in either the acid SH or base S^- state)

(B)

Fig. 1. (A) The B2AR model as viewed through the plane of the cell membrane (TM3 is the center solid red ribbon). A includes the initial docking position of epinephrine (EPI) as a representative ligand. Ligands were manually docked in the acid receptor state with no initial refinement of the side chains. The space-filled residue at the top is the highly conserved cysteine residue C106 (C3.25 or CysIII:01), which provides a free sulfhydryl or thiol group (yellow) in either an acid or base state (SH or S^-). The space-filled residues at the bottom are the critical DRY region near the intracellular end of the receptor. (B) The sequences for this B2AR model are refined from "What-IF" structures proposed by Vriend (http://www.gpcr.org/7tm/models/vriend2/index.html) and based upon Baldwin et al.'s model [20]. The C106, in which the sulfhydryl group was modeled in either the acid, SH; or base, S^-, state, is labeled in TM3. The two mutants, D113E and D130A, which occur in TM3, are listed below the sequences.

program QUANTA. Each ligand model was constructed with the chirality corresponding to the most active form. The models for epinephrine and norepinephrine had chirality R and the model for pindolol had chirality S. Charges were determined from calculations with the program GAUSSIAN-98 using 6–31G* basis sets with the Hartree–Fock method. Energy minimization and molecular dynamics calculations were done by using the set of programs CHARMM (version 24).

The ligand was docked into the acid form of the receptor with the cysteine in the acid state (SH) using facilities of the program QUANTA. The ligand was positioned near enough to form a salt bridge with either the aspartate D113 in the wild type receptor or the glutamate E113 in the D113E mutant receptor. The position of the ligand in the acid state was also used as the starting position for docking in the base state (S^-).

Subsequent calculations and molecular dynamic simulations were done with the C106 in either the uncharged SH (acid) or charged S^- (base) state. Initial receptor minimization included sequential intervals of steepest descent, conjugate gradient, and adopted basis Newton–Raphson. The dynamics calculations included heating to 310 K (30 ps), equilibration (50 ps), and simulation (200 ps) portions. The lengths of the bonds involving hydrogen atoms were constrained according to the SHAKE algorithm, allowing an integration time step of 0.001 ps. Integration of Newton's equation of motion was done by using the Verlet algorithm.

Harmonic constraints with a force constant of 0.5 were applied in order to maintain the structure of the receptor backbone. A dielectric constant of 4.0 was used to emphasize electrostatic interactions between the ionized cysteine and the rest of the receptor since the electrostatic interactions computed generally take place within the protein interior in the absence of intervening solvent. A cut-off distance of 60 Å was used to model the distant interactions between the ionized cysteine and the rest of the system. Equilibration was observed after 50 ps for all runs. For each run, the minimized average structures used for the analyses were taken from the last 5 ps of the simulations.

Sixteen molecular dynamics (MD) simulations were analyzed for this study comprising eight acid–base pairs with the C106 cysteine in either the SH or S^- states. The MD simulations included the wild type (WT), and two mutant B2ARs with and without bound ligands as described in Table 1. These include each of the following receptor systems in acid and base states: the wild-type (WT) B2AR alone and with the ligands epinephrine (EPI), norepinephrine (NE) and pindolol (PIN); the D113E mutant alone and with the ligands NE and PIN; the D130A mutant alone.

We understand that this B2AR model without loops, in vacuum, with backbone restraints may not completely validate a GPCR activation hypothesis, but hope that it will be considered in the larger context of the experimental and theoretical data that it attempts to explain.

2.2. The calculation of interaction energies

For each of the base and acid states of a particular receptor system the interaction energy (ΔE) was calculated for each molecular complex by taking the energy of the receptor–ligand molecular complex (E_{RL}) and subtracting the energies of the free receptor and ligand molecules (E_R) and (E_L) respectively:

$$\Delta E = E_{RL} - E_R - E_L \quad (3)$$

In general, the lower or more negative the interaction energy the more favored the formation of the molecular complex.

Each of the interaction energies can be further partitioned into Lennard–Jones (LJ) and electrostatic (EL) terms according to the expression:

$$\Delta E = \Delta E^{LJ} + \Delta E^{EL} \quad (4)$$

The differences between interaction energies ($\Delta\Delta E$) for various molecular complexes were calculated as before [16] where the ΔE^{EL} differences for the base minus the acid states (B − A) of a ligand–receptor complex is calculated as:

$$\Delta\Delta E^{EL} = \Delta E^{EL}(B) - \Delta E^{EL}(A) \quad (5)$$

All of the interaction energies were calculated from the average structures generated from the last 5 ps of the MD simulations.

Table 1
CHARMM energy differences for the base–acid receptor states

	Receptor	Ligand	ΔE (kcal/mol)	ΔLJ[a]	ΔEL[b]	ΔIE[c]
System						
WT	WT	None	+33.9	+10.4	+15.7	7.8
WT + EPI	WT	EPI	−3.8	−8.7	−5.1	10.0
WT + NE	WT	NE	−10.6	−9.0	−3.6	2.0
WT + PIN	WT	PIN	+7.7	+10.4	+3.6	−6.3
Mutants						
D113E	D113E	None	+10.4	−5.9	+0.9	0.5
D113E + NE	D113E	NE	−8.3	−10.6	+0.6	1.7
D113E + PIN	D113E	PIN	+12.3	+5.0	+6.8	15.4
D130A	D130A	None	+10.6	+13.1	−0.1	−2.4

[a] ΔLJ = the energy difference between the base and acid states for the Lennard–Jones energy terms (kcal/mol).
[b] ΔEL = the energy difference between the base and acid states for the electrostatic energy terms (kcal/mol).
[c] ΔIE = the energy difference between the base and acid states for the internal energy terms (bending, stretching and torsional) (kcal/mol).

3. Results

3.1. Differences between the acid and base states

Fig. 2A and B displays the electrostatic potentials for the acid and base states of the B2AR plotted for the positive (blue) and negative (red) potentials. These figures all have the same orientation as the B2AR model displayed in Fig. 1. Fig. 2A and B show that the transition of C106 from the uncharged acid state (RSH) to the charged base state (RS^-) produces a change from an electrophilic (blue) to a more nucleophilic (red) state. This is consistent with the base state (RS^-) preferentially attracting the positively charged cationic amine group of binding ligands and thereby creating a higher affinity state consistent with previous results [16].

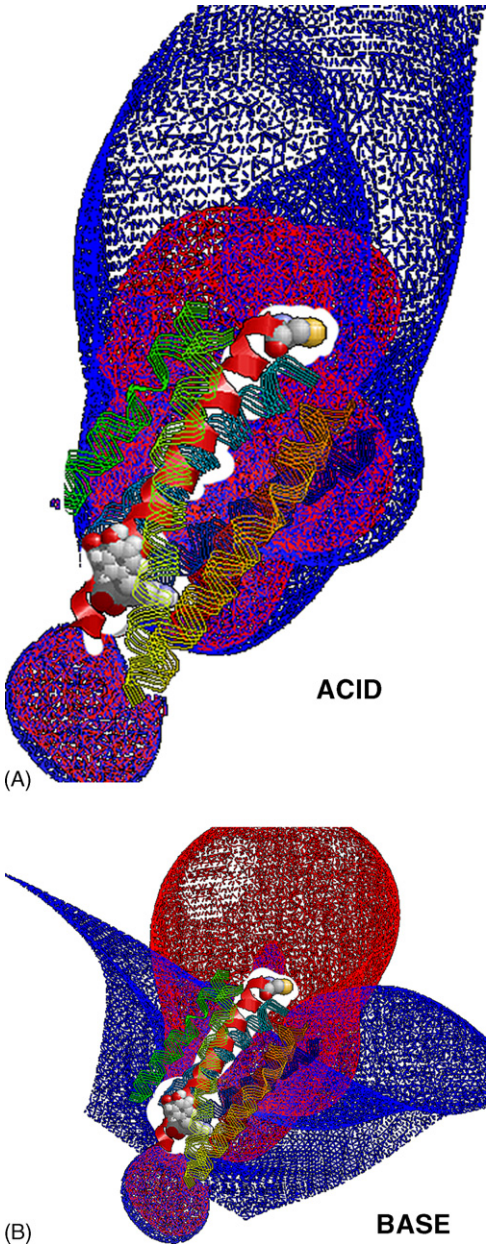

Fig. 2. (A) Plot of the acid state with the same orientation as shown for the B2AR model in Fig. 1A with the extracellular end at the top of the picture and TM3 as the solid red ribbon. The space-filled residue at the top is the highly conserved cysteine residue C106 (C3.25 or CysIII:01), which provides a free thiol group (yellow) in an acid–base equilibrium between uncharged (RSH) and charged (RS^-) states. The space-filled residues at the bottom are the DRY region near the intracellular region of the B2AR. The electrostatic potentials are plotted as positive 25 (blue) and negative −25 kJ mol^{-1} (red) meshes in both A and B. The acid state corresponds to the uncharged RSH or "R" receptor state in this model. (B) Plot of the base state with the same orientation as shown for the B2AR model in Fig. 1A and the acid state in A. The base state corresponds to the charged RS^- or "R^*" receptor state. Portions of these composite pictures were generated with the Swiss-PdbViewer (from Ref. [51]).

After performing the MD simulations representing a composite of several molecular structures that exist around the equilibrium energy, we analyzed various properties of the average structures. Fig. 3 displays the root mean square deviations (RMSDs) for the acid and base differences of the conserved residues in the wild type B2AR (labeled "*") together with those residues displaying a RMSD greater than 1 Å. Except for the arginine R3.50 (R131), the other conserved residues show less than 1 Å difference. This suggests that these residues may function as a scaffold that is not as dynamically mobile as other parts of the B2AR.

The distances between the alpha carbons of R131 and D130 in TM3 and the alpha carbons of the residues within the other helices were generally shorter in the acid than in the base state suggesting that the base structure is somewhat larger than the acid structure (not shown).

The distance between the R131 and D130 alpha carbons in the DRY region may also be affected by the strength of the salt bridge and the loss of this stabilizing interaction in the base state as discussed below.

If the extra negative charge in the base state shows a higher affinity for the positively charged agonist ligands, then we must nevertheless explain why antagonist ligands do not favor the base over the acid receptor state. In order to understand this, we analyzed the acid–base interaction energy differences of the average molecular structures in more detail.

The CHARMM energy differences for the WT, D113E and D130A B2AR mutants are displayed in Table 1 for the base minus acid difference (B − A). Apart from the extra negative charge on the thiol group, the base state of the WT B2AR has a higher overall CHARMM energy than the acid state (see ΔE(B − A), Table 1).

In both the D113E and D130A mutant receptors, the base state also has a higher CHARMM energy than the acid state although the total energy change, ΔE(B − A), is less than that for the WT B2AR. The higher energy of the base state in the WT and the mutant B2ARs may be partly attributed to the repulsion energy between the negative charge on the ionized sulfhydryl group (RS^-) and the other negatively charged regions such as the backbone oxygens and the carboxyl group of D113, which is two helical turns (about 10.8 Å) away from the cysteine C106. Overall, the total CHARMM energy profile suggests that the acid state is energetically more favored than the base state in the unliganded native conformation, which is expected if the native receptor exists primarily in an off conformational state.

For the agonist-bound receptors in almost all cases, the difference in the CHARMM energies favors the base state over the acid state, whereas the antagonist pindolol PIN showed an energy pattern that is contrary to this. This may be partially due to a larger ΔLJ(B − A) energy difference for PIN compared to the agonist ligands (see Table 1).

For the D113E and D130A mutant receptors, there is a lower energy difference compared to the that for the WT receptor alone (compare ΔE(B − A) 33.9 with 10.4 and 10.6 kcal/mol in Table 1). Interestingly, the overall CHARMM energy differences for these mutations are very similar but result from differing intramolecular forces. For the D130A mutant, the CHARMM energy of the ΔEL(B − A) difference decreases dramatically from 15.7 to −0.1 kcal/mol. In contrast, the D113E mutant shows CHARMM energy differences for the base minus acid states (B − A) that result from each of the separate energy terms ΔLJ, ΔEL, ΔIE and ΔE as shown in Table 1. These

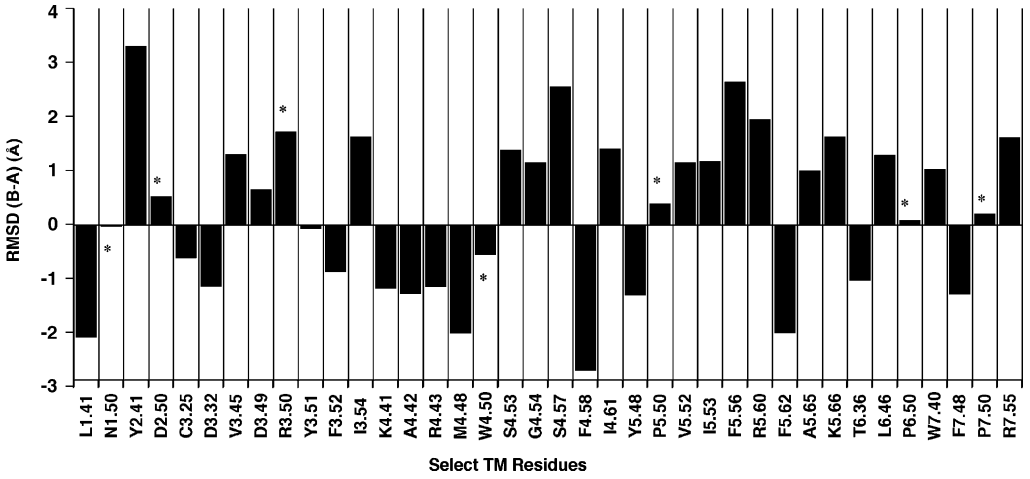

Fig. 3. The differences in the root men square deviation (RMSD) for the base minus acid states (B − A). The residues are listed as for the Ballesteros and Weinstein notation [52]. Conserved residues 1.50, 2.50, 3.50, 4.50, 5.50, 6.50 and 7.50 are starred "*". The other residues are either residues of interest such as the DRY region or those residues with the RMSD(B − A) ≥ 1 Å.

observations suggest that there may be a lower energy barrier for the overall acid to base transition for these mutant B2ARs resulting from different molecular interactions.

For the unbound wild-type receptor, the transmembrane (TM) domain interaction energies for the base minus acid states (B − A) are plotted in Fig. 4 for all possible TM pairs. These energy differences range from a low of −3 kcal/mol for TM2 × 3 to a high of 18 kcal/mol for TM6 × 7 followed closely by 16 kcal/mol for TM3 × 4.

The largest total energy changes occur in TM6 × 7 and TM3 × 4 followed by TM3 × 6, TM1 × 7 and TM3 × 5 (Fig. 4). The largest changes in the electrostatic energy (ΔEL) occur for the TM3 × 4 and TM6 × 7 interactions; whereas, the largest changes in the Lennard–Jones energy (ΔLJ) occur for the TM3 × 6 and TM6 × 7 interactions (Fig. 4).

This suggests that these major helical interactions are perturbed by the transition from an acid to base receptor state apart from any ligand binding. TM7 also appears to be strongly

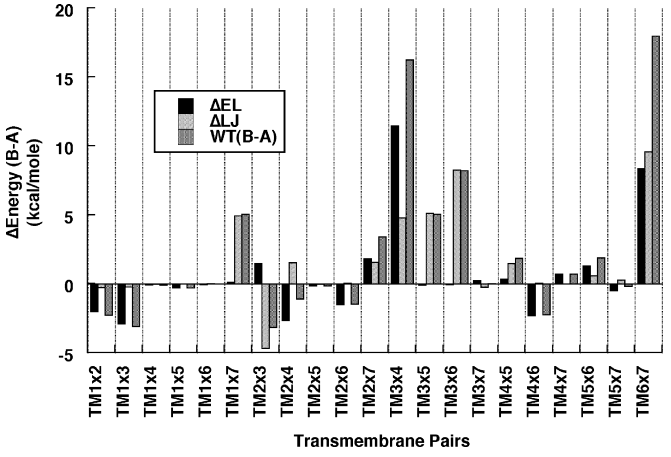

Fig. 4. Transmembrane domain interaction energy differences for the WT B2AR receptor displayed for the differences between the base and acid (B − A) states. The total energy differences for all TM pairs is displayed as the base minus acid (B − A) and is also broken down into the separate van der Waals (ΔLJ) and electrostatic (ΔEL) interactions.

connected indirectly through the electrostatic interactions between TM6 and TM7. These interactions demonstrate the complex dynamics associated with the acid to base transition.

3.2. Differences in interaction energies and their correlation with ligand efficacies

The smaller ligands have a larger positive charge density and a more favorable interaction with the negatively charged cysteine in the base state suggesting that their relative efficacies may be related to their charge densities and their ability to interact with the base receptor state [16].

The CHARMM energy differences, ΔE(B − A), for the ligands EPI, NE, and PIN bound to the WT receptor are −3.8, −10.6, and +7.7 kcal/mol, respectively (Table 1). When norepinephrine and pindolol are bound with the D113E mutant receptor, the values of the CHARMM energy difference are −8.3 and 12.3 kcal/mol, respectively (see the ΔE(B − A) values for D113E + PIN and D113E + NE in Table 1). A partial explanation may be that for the NE and PIN ligands complexed with the D113E mutant receptor, the average distances between the ligands and the receptor increase in comparison with those in the wild-type complexes, which may be due to the slightly longer sidechain on the glutamate residue in the D113E mutant.

The RMSDs were calculated for the acid and base states of the unbound receptor state and the ligand-bound receptor. The greatest RMSDs occur within TM6 and are greater for the full agonists, EPI and NE, than for the antagonist, PIN (not shown).

However, we could not consistently connect the RMSDs of any specific residue to the experimental ligand efficacies. Although TM7 showed a larger RMSD with PIN in the D113E mutant than in the WT receptor (not shown), this may be partially attributed to the displacement of PIN by the larger glutamate residue, which places the ligand closer to TM7.

In contrast, the electrostatic interaction energies ($\Delta\Delta E^{EL}$) show that PIN in the D113E mutant receptor has a larger $\Delta\Delta E^{EL}$ than for PIN bound to the WT B2AR. One reason for this may be that the basic nitrogen of PIN is closer to C106, which

Table 2
Electrostatic interaction energy differences for the base minus acid states with the percent sodium fluoride activity

Receptor system	$\Delta\Delta E^{EL}$ (kcal/mol)	NaF[a] (%)
WT + EPI	−14.0	95
WT + NE	−14.4	95
D113E + NE	−5.5	50
D113E + PIN	−6.4	35
WT + PIN	−4.7	0

[a] These values were taken from Strader et al. [19]. The correlation coefficient for $\Delta\Delta E^{EL}$ vs. %NaF is $r = 0.92$.

Table 3A
Changes in key transmembrane domain interaction energy differences for the base minus acid states

Receptor systems (B − A)	TM pair energies (kcal/mol)			
	TM1 × 7	TM3 × 4	TM3 × 6	TM6 × 7
WT + EPI	−7.3	−23	−7.7	−5.7
WT + NE	−3.2	−2.7	3.8	−6.1
D113E + NE	1.3	−0.5	2.2	−4.5
D130A	−2.7	−6.4	4.8	1.6
D113E + PIN	1.7	−0.4	−1.3	1.7
WT + PIN	1.4	7.1	3.8	5.4

generates a larger $\Delta\Delta E^{EL}$ in the D113E mutant. As a result, the electrostatic interaction energy of PIN with the negatively charged C106 residue is greater, which provides an explanation for the increased efficacy of pindolol as primarily due to the increased electrostatic favoring of the base state in the D113E mutant.

The calculated $\Delta\Delta E^{EL}$ energies for WT + PIN were −4.7 kcal/mol versus −6.4 kcal/mol for the D113E + PIN, which are in good agreement with the experimentally observed increase in the experimentally measured percent sodium floride activity as shown in Table 2.

For the wild-type receptor with the NE ligand, the calculated $\Delta\Delta E^{EL}$ was −14.4 kcal/mol; whereas for the D113E mutant receptor with NE, the $\Delta\Delta E^{EL}$ was −5.5 kcal/mol suggesting a diminution in the efficacy of NE in the mutant consistent with previous experimental findings [19] (see Table 2). These findings are consistent with the observations from Strader's group that the D113E mutation changes PIN from an antagonist to a partial agonist and reduces the activity of NE to that of a partial agonist [19].

In order to further understand the effects of ligand occupancy on the B2AR, we examined the transmembrane (TM) interaction energy differences for the acid and base states in the EPI bound WT receptor. In general, the binding of EPI changes the interaction energy differences of he base minus acid states (B − A) from positive to negative for the TM1 × 7, TM3 × 4, TM3 × 6 and TM6 × 7 interactions (see Fig. 5A). This suggests that one of the actions produced by EPI binding is to increase the magnitude of the TM interactions between TM1 × 7, TM3 × 4, TM3 × 6 and TM6 × 7 in the base state of the receptor. Many of these interactions have been previously linked either directly or indirectly to receptor activation [9–15].

With the WT B2AR bound EPI, the TM3 × 4 interaction energy changes from a positive 16 to a negative 23 kcal/mol suggesting that there is a closer interaction of TM3 and TM4 in the base state. The TM3 × 4 interaction is also the largest interaction measured for all of the EPI induced interaction energy changes shown in Table 3A.

The interdomain interaction energy differences for the antagonist PIN in the WT receptor show an opposite pattern from the EPI and other activating ligands (compare Fig. 5A and F and Table 3A). Although PIN binding reduces the positive interaction energy differences for TM1 × 7, TM3 × 4, TM3 × 6 and TM6 × 7, PIN fails to make them negative. This suggests that the weaker electrostatic interaction energy change ($\Delta\Delta E^{EL}$) for the PIN binding translates into TM interaction energy changes that fail to reach a critical threshold value for receptor activation. This may be a key difference between the antagonist and agonist ligands.

For the mutant D113E + PIN receptor system, TM3 × 4 and TM3 × 6 become negative suggesting an activating pattern that is supported by previous experimental observations showing partial agonist activity [19,40]. From this analysis, TM3 × 4 changing from positive to negative emerges as a consistent predictor for all of the activating ligands and mutations in this study.

To further isolate the effects of ligand binding, we subtracted the TM energy differences of the WT(B − A) from the other receptor systems in order to see the net effect of the bound ligands. These results are displayed in Table 3B. This highlights those differences created by ligands or mutations that change the TM energy patterns of the unbound WT B2AR.

By this analysis, the largest effect of EPI binding is more readily seen for the TM3 × 4, TM6 × 7, TM3 × 6 and TM1 × 7 interdomain interaction energies (Table 3B). These changes are largely consistent with the TM interaction energies in Table 3A, but more clearly demonstrate that the net effect of ligand binding centers around the major TM3 × 4, TM6 × 7, TM3 × 6 and TM1 × 7 interactions.

In the receptor systems with the largest agonist activity, the TM3 × 4 and TM6 × 7 interactions are also the largest (Table 3B). The pattern of TM interaction energies for the mutant D130A receptor compared to the EPI bound WT receptor also displays a strong correlation ($r = 0.90$ in Fig. 6) suggesting that this may be a general pattern for both ligand and constitutive receptor activation. These general patterns support Christopoulos and Kenakin's concept of protean

Table 3B
Changes from the wild-type B2AR in key transmembrane domain interaction energy differences for the base minus acid states

Receptor systems (B − A)	TM pair energies (kcal/mol)			
	TM1 × 7	TM3 × 4	TM3 × 6	TM6 × 7
EPI-WT	−12	−39	−16	−24
NE-WT	−8	−19	−4	−24
D113E + NE-WT	−4	−17	−6	−22
D130A-WT	−8	−23	−4	−16
D113E + PIN-WT	−3	−17	−10	−16
PIN-WT	−4	−9	−4	−13

agonism by demonstrating that there exist similar activation patterns that vary around a common theme for activating ligands and mutations [41].

These findings also demonstrate that although pindolol is an antagonist, it contains some elements, albeit weaker, within its interaction pattern in common with the full agonist epinephrine. Parts of these patterns may represent energies that fail to reach a threshold energy change for receptor activation since the PIN energy differences in Table 3B are generally smaller than those for the agonist ligands.

However, in the D113E mutant receptor, the antagonist pindolol changes to a partial agonist and norepinephrine activity decreases approximately 50% to that of a partial agonist. This occurs in our analysis by the alteration of key TM domain interaction energies such as the changes in the TM3 × 4 and TM3 × 6 for PIN (compare Fig. 5D and F) and those for the TM3 × 4 and TM6 × 7 for NE (compare Fig. 5C and B).

In contrast, the accompanying changes to the TM domain interaction energy differences for D113E + PIN compared to WT + PIN show a more negative energy pattern for the TM3 × 4, TM3 × 6 and TM6 × 7 interactions in the D113E mutant consistent with a higher activity for PIN in this mutant (Tables 3A and 3B).

If the constitutively active mutant D130A is assumed to have approximately the same activity as the D113E + PIN system, then the TM6 × 7 interdomain interaction energy differences listed in Table 3B correlate well with the experimentally measured relative intrinsic efficacies listed in Table 2 (%NaF). Interestingly, there is also a good correlation between all of the other ligand bound and mutant receptors with their experimentally reported activities ($r = 0.94$ with the D130A, or $r = 0.92$ without the D130A mutant).

3.3. Regions within the receptor that may have a role in signal recognition and transmission

In our model, C106 is two-helical turns (∼10.8 Å) above the important aspartate residue D113 that forms a counterion with the protonated amine of catecholamine ligands. This is

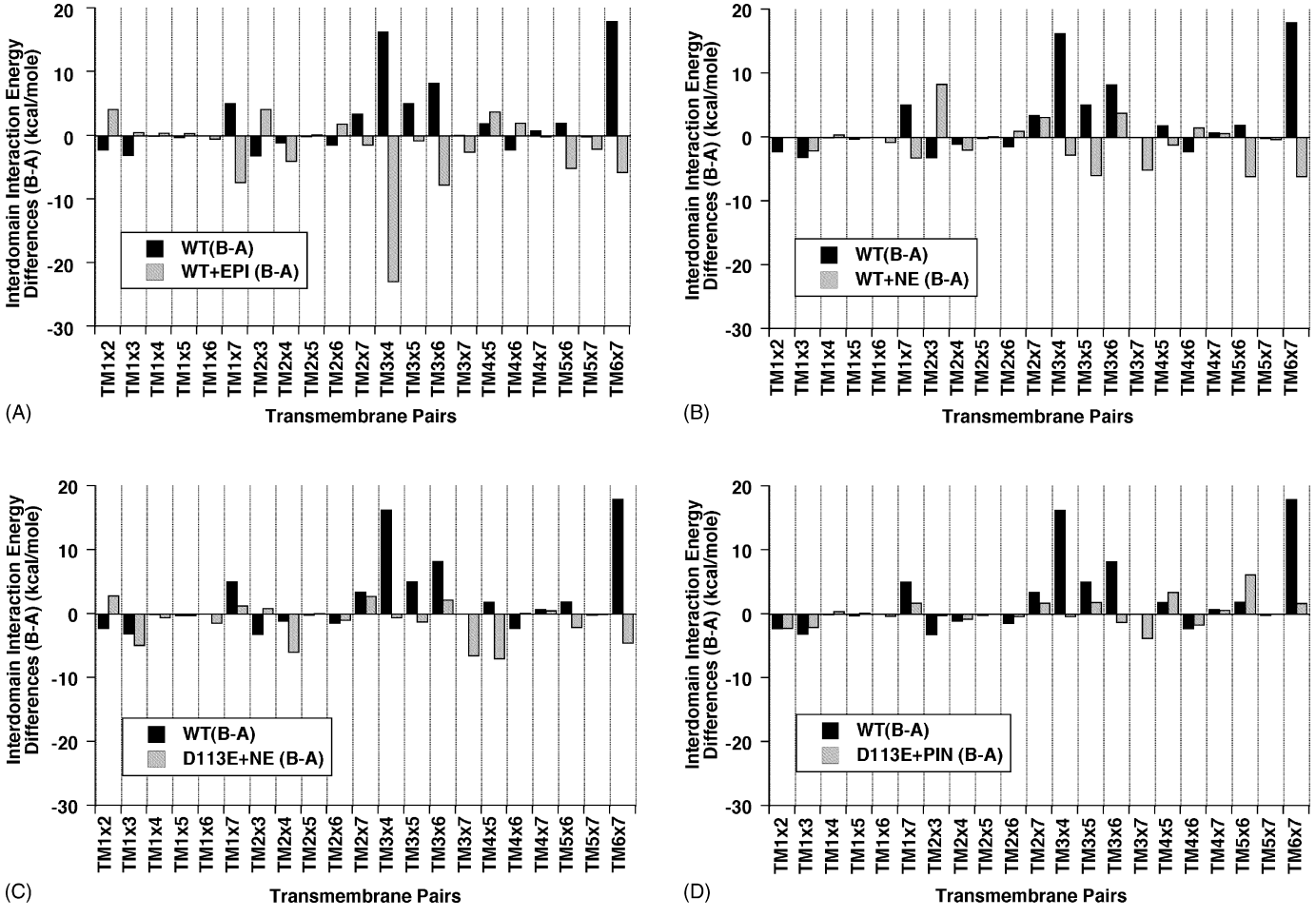

Fig. 5. (A–G) The transmembrane domain (TM) interdomain interaction energy differences for the base minus the acid (B − A) states for all possible TM domain pairs. In all parts, the vertical scales are equal. Each figure shows the patterns of the transmembrane domain (TM) interdomain interaction energy differences for the base minus the acid (B − A) states with the unliganded wild-type B2AR WT (B − A) in the black bars given for comparison. A shows epinephrine with the wild-type receptor (WT + EPI (B − A)). B shows norepinephrine with the wild-type receptor (WT + NE (B − A)). C shows norepinephrine with the D113E mutant (D113E + NE (B − A)). D shows pindolol with the D113E mutant (D113 + PIN (B − A)). E shows the D130A mutant (D130A (B − A)). F shows pindolol with the wild-type receptor (WT + PIN (B − A)). G shows the D113E mutant (D113E (B − A)).

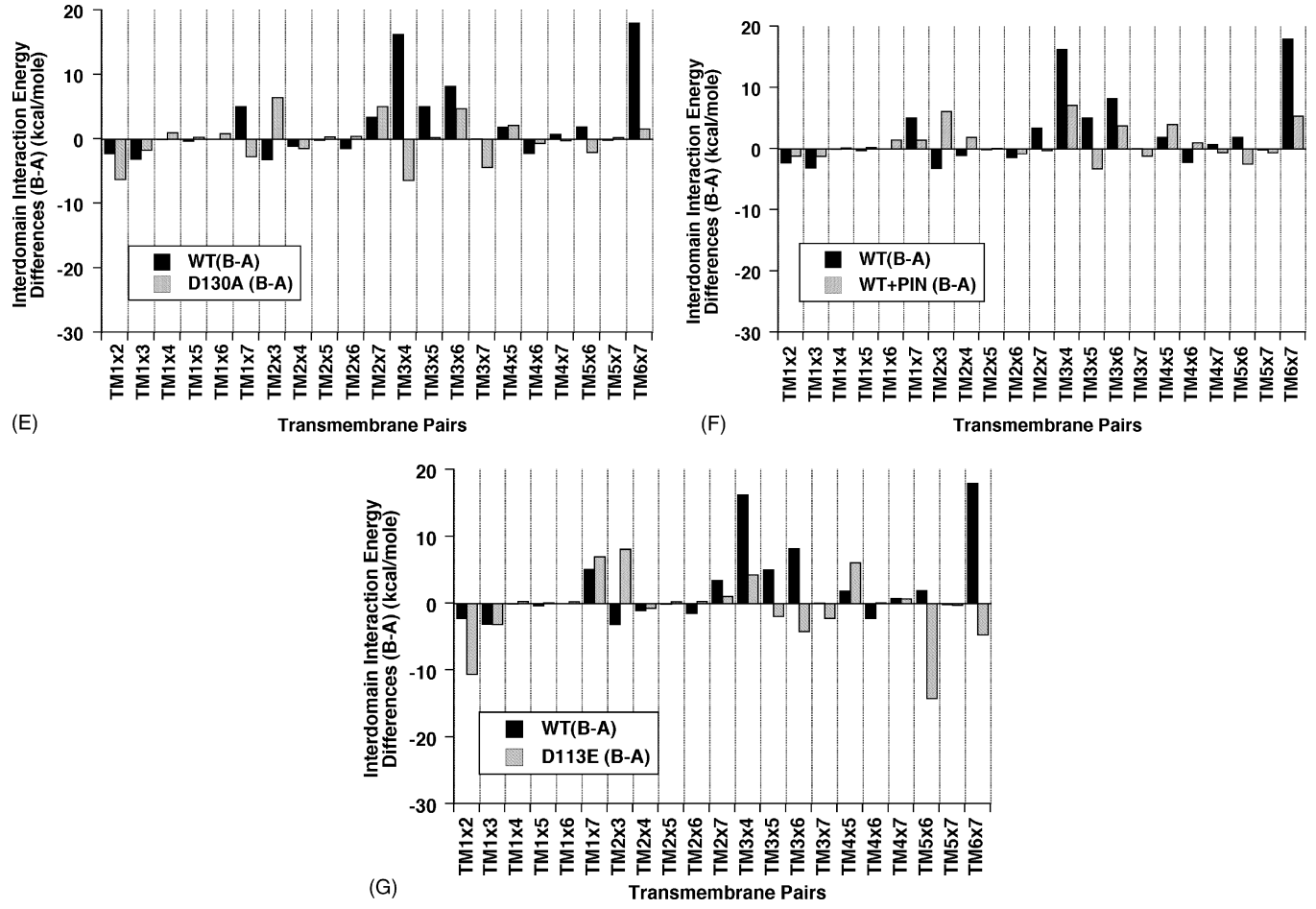

Fig. 5. (*Continued*).

consistent with Heinonen et al.'s, suggestion that a reactive cysteine or thiol group is 8.6–14.5 Å from the Asp113 in the α_2-adrenergic receptor [30]. Similarly in rhodopsin, the distance from retinal to the glutamate E134 in the ERY region is between 19 and 30 Å (PDB 1F88) [22], which generally agrees with the distances for ligands docked within our B2AR model.

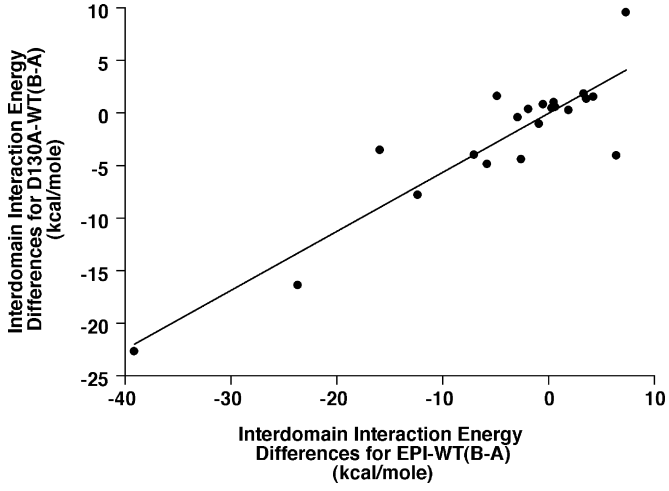

Fig. 6. Correlation of the TM interdomain interacton energy differences of the base minus acid states for the constitutively active mutant D130A vs. the wild-type B2AR bound with epinephrine (D130A-WT(B − A) vs. EPI-WT(B − A); $r = 0.90$).

The protonation and movement of R131 (R3.50) has been previously suggested as a potential mechanism for receptor activation [13,40,42]. Previously in the two-state acid–base model for the 5-HT2A receptor, the charged cysteine was observed to have long range electrostatic interactions with the aspartate and arginine residues within the DRY region [16].

In the present study, the acid to base change of C106 is accompanied by a corresponding displacement of the aspartate and arginine in the DRY region of the B2AR (0.7 and 1.7 Å, respectively) (Fig. 3). This demonstrates that the acid to base transition perturbs R131 enough to disrupt this bonding. This suggests that deprotonation of C106 followed by a separate protonation of R131 may be a feasible molecular mechanism for the transmission of an extracellular signal to the intracellular side of the receptor.

All of the possible pairs of TM domain interaction energy differences demonstrate complex patterns for both the electrostatic (ΔEL) and Lennard–Jones (ΔLJ) interactions as shown in Fig. 4 for the wild-type B2AR. The largest perturbations occur for the ΔEL energies of the TM3 × 4 and TM6 × 7 interactions and the ΔLJ energies of the TM3 × 6 and TM6 × 7 interactions.

For all of the MD simulations, the most consistent change accompanying receptor activation is the change of the TM3 × 4 interaction energy from positive to negative together with the $\Delta\Delta E^{EL}$ becoming more negative. This is observed for all of the active systems we studied; WT + EPI, WT + NE, D113E + NE, D130A and D113E + PIN, shown in Fig. 5A–E. These TM domain interactions may in turn affect the second and third intracellular loops (ICL2 and ICL3), which are considered to be important in receptor-G protein-coupling [15,30]. These interactions may produce a repositioning of the arginine in the polar pocket surrounding the DRY region demonstrating that our relatively simple model generates complex electrostatic and conformational changes within the B2AR that link TM changes to previously recognized patterns of receptor activation [5,13,21,40].

4. Discussion

This work tests a two-state acid–base model for an ionizable cysteine residue found within all GPCRs. This cysteine is strategically located two-helical turns or about 10.8 Å above the important aspartate residue D113 in TM3 that forms a counterion with the protonated amine of catecholamine ligands in adrenergic receptors [30]. The acid–base transition of this cysteine, C106 in the B2AR, modulates the internal energies of the receptor and the interaction energies of various ligands that interact with the B2AR in ways that correlate well with previously observed transmembrane domain interactions and the experimentally measured ligand efficacies (Table 2 and Fig. 6). Although it would be preferable to have a larger sampling of ligands with their experimental efficacies, these simulations taken together with previous studies suggest that those ligands that activate the B2AR also show a preferential electrostatic attraction for the base form of the receptor state [16].

Previous two-state models for GPCR activation have been considered to represent a simplification of the available conformational space [2,43]. However, single-molecule spectroscopy of the B2AR receptor has recently suggested that there are two distinct states with a population enrichment of one state occurring when bound with agonist molecules [43]. The authors of this study suggested that there is a population of active receptor states that are separate from the active states in the native receptor, which appears contrary to the findings from Bond et al. [1].

One possible way to resolve these seemingly contradictory findings is through the interpretation that our two-state model provides that allows for a net enrichment of the active state through either receptor overexpression or ligand binding [6–8].

On the molecular level, we have determined that the discrete molecular states RSH and RS^- connect the mathematically general R and R^* states to electrostatic interaction energy changes ($\Delta\Delta E^{EL}$) that closely correlate with their experimentally measured ligand efficacies as seen previously for the 5-HT2A receptor [16]. This suggests a molecular basis for the R to R^* shift in the receptor equilibrium as a measure for the net receptor response and supports the concept that cysteine modulation of ligand binding may be an important mechanism to explain how ligands activate these receptors [16].

Although this picture may be more complex than previously characterized, the acid–base transition of C106 clearly creates energy perturbations that are largely compatible with many previous experimental findings [9–15]. In the unliganded wild-type B2AR, the TM1 × 7, TM3 × 4, TM3 × 5, TM3 × 6 and TM6 × 7 interactions are all strongly positive for the unbound WT (B − A) states of the B2AR (gray bars in Fig. 4 and the black bars in Fig. 5A–G). However, these interactions switch from positive to negative upon the binding of epinephrine with a rank order of TM3 × 4 > TM6 × 7 > TM3 × 6 > TM1 × 7 (Fig. 5A).

In addition, the TM3 × 4 interaction also changes from positive in the unbound D113E mutant to negative in the PIN bound D113E mutant, which suggests a possible threshold activation energy for this interaction (compare Fig. 5G with D). All of the MD simulations of the receptor systems experimentally shown to be active, WT + EPI, WT + NE, D113E + NE, D130A and D113E + PIN, consistently show that the TM3 × 4 interaction energy changes from a positive to negative value (Table 3A). Although more work needs to be done to support this finding, at least one study has implicated TM4 in the activation of the M1 muscarinic receptor [44].

One of the more subtle changes involves the D113E mutation that changes pindolol from an antagonist in the WT B2AR to a partial agonist in the D113E mutant [19]. To our knowledge there have been no other theoretical models that have explained this experimental finding. However from our simulations, the change from an aspartate to glutamate creates a larger difference in pindolol's interactions between the acid and base states, which is directly reflected in the $\Delta\Delta E^{EL}$ energy difference and the changes in the TM interaction energies. This is most evident by the TM3 × 4 and TM3 × 6 interactions, which change from positive for the WT + PIN to negative for the D113E + PIN system (compare Table 2 and TM3 × 4 and TM3 × 6 in Fig. 5D and F).

Unlike the agonist ligands in the wild-type B2AR, pindolol fails to make the TM3 × 4, TM6 × 7, TM3 × 6 and TM1 × 7 interaction energies negative, which represents a crucial difference between the agonist and antagonist ligands. This molecular mechanism elucidates these subtle changes within the dynamic patterns of B2AR activation.

Further experimental observations suggest that some ligand-dependent conformations favor one particular G protein over another as a basis for protean agonism [2]. Although EPI and NE are about equally effective at activating the B2AR, their TM interactions show some unique differences. For the NE bound B2AR, all of the major TM interactions except for TM3 × 6 change from positive to negative; whereas for the EPI bound receptor the TM3 × 6 also changes from positive to negative (Fig. 5A and B). However, their overall TM changes show similar patterns and display a strong correlation relative to the acid–base changes of the WT receptor ($r = 0.83$).

These common patterns are comprised of changes in the TM1 × 7, TM3 × 4, TM3 × 6 and TM6 × 7 interaction energy differences (Tables 3 and 4). Interestingly, the constitutively

active mutant D130A also displays a similar pattern of TM interactions compared to the EPI bound receptor suggesting a common pattern for receptor activation (Figs. 5A and E and 6). This supports the concept that protean agonism arises naturally from ligand or mutation specific patterns due to variations in internal interaction energies that may favor receptor binding to one particular G protein over another.

In comparison with rhodopsin, Sakmar et al. implicated the H-bond networks linking the TM1 × 7, TM3 × 4, TM3 × 6 and TM6 × 7 interactions to receptor activation [15] and Ballesteros et al. showed that the charge-neutralizing mutation of D130 in TM3 of the B2AR to asparagine (D130N) led to a significant increase in basal and pindolol-stimulated cAMP accumulation, which was thought to be due to an increase in the relative motions of TM3 to TM6 [13,14]. In the context of our model, these TM interaction changes arise from the acid to base transition alone.

The ‘‘protonation hypothesis’’ for B2AR activation suggests that the protonation of the aspartic/glutamatic acid residue in the D/ERY portion of the cytoplasmic side of TM3 is a key event for initiating receptor activation [21]. The constitutively active D130A mutation is thought to free the arginine R131 or R3.50 within the critical DRY region [14,40], which suggests that the protonation of the D130 or D3.49 frees this arginine to move out of the polar pocket [13]. This is also supported by the experimental finding that in isolated B2AR membrane preparations decreasing pH favors receptor activation in vitro [45].

In the context of our model, the existence of at least two different pH-sensitive residues on both interior and external sides of the receptor may complicate these interpretations since another study has shown that an increase in external pH increases receptor activation [46]. This still raises the important question of how activating ligands that bind to the extracellular region might induce the protonation of acidic residues on the cytoplasmic side of the receptor. In our model, the aspartate and arginine within the DRY region move by 0.7 and 1.7 Å (Fig. 3), which may be enough to disrupt an intramolecular bond such as a salt bridge. This would reconcile the observations that either an acidic or basic pH may promote receptor activation, since the differing pH-sensitivities of the two residues Cys 106 or Asp 130 may be involved on both the extracellular and intracellular side of the receptor in the cell membrane.

Recent experimental observations of receptor dimerization together with parallel receptor activation studies demonstrate that receptor dimer formation enhances receptor activation [47,48]. Zeng and Wess produced the first direct evidence for the existence of muscarinic receptor dimers formed from two conserved cysteine residues, C140 and C220 located on the extracellular side of the receptor with C140 corresponding to C106 of the B2AR [47].

In the dopamine D2 receptor (D2R), Javitch and co-workers showed that the site of crosslinking occurs at C168 on the extracellular end of TM4 and concluded that cross-linking does not impair the ability of dopamine to activate the D2AR, demonstrating that the receptor can bind dopamine and activate G_i with a disulfide bond between the C168 residue in each subunit of the dimer [49]. These observations suggest that the active receptor state remains within the receptor dimers *themselves*.

The possible role for a dimeric species in B2AR signaling was discovered when it was found that receptor ligands affect the monomer:dimer equilibrium [48]. Isoproterenol increased the relative amount of dimer by 45% and also protected the dimer from the disruptive effect of the TM6 peptide [48]. These results suggest that isoproterenol stabilizes the B2AR dimer even in the absence of G proteins, which is compatible with our model.

For any particular redox environment, there necessarily occurs an equilibrium between disulfide bonds and free sulfhydryls, which are then free to be influenced by the environmental pH. If two receptors dimerize by forming a disulfide bond, they will necessarily produce a pair of free sulfhydryls, because the four cysteine residues of the two disulfide bonds form only a single disulfide bond, thereby leaving two sulfhydryl groups free. This is a chemical disproportionation reaction that happens when a substance can be simultaneously oxidized and reduced, thereby allowing the formation of free sulfhydryl groups.

We tested an extension of our previous model [16] in the larger context of past modelling efforts. Although this B2AR model without loops, in vacuum, with backbone restraints may not completely validate a GPCR activation hypothesis, our model offers a potentially powerful approach to modelling two-state interactions as the differences in interaction energies. These simulation results provide new insights into the relationships observed between selected biochemical data and the structural interactions that occur during receptor activation.

In summary, these findings place the activation of the B2AR into a dynamic and general molecular model that explains many aspects of how ligands or mutations alter the B2AR to produce activation. These findings generally support Kenakin’s concept of protean agonism through a mechanism that describes ligand biased conformational change and suggest that there are multiple ways to activate and allosterically modulate the B2AR [2,50]. This model also relates the transmembrane domain motions of GPCRs to explicit receptor states and demonstrates that many elements from several different models may be important parts of a bigger view of receptor activation. Hopefully, this work will cultivate an appreciation for receptor function in terms of a general, two-state acid–base model that will present fruitful alternatives for the modeling of GPCR activation in the future.

5. Conclusions

The major conclusions from this work are:

(1) The electrostatic interaction energy changes correlate well with the experimentally observed ligand efficacies.
(2) The interaction energy changes for the helical/transmembrane domain interactions are generally compatible with previously described events for GPCR activation.
(3) This molecular model ties together many experimental and theoretical findings observed for the B2AR and other GPCRs.

Acknowledgments

The authors express their gratitude to Drs. Harel Weinstein and Roman Osman for their encouragement and support. Many thanks to Dr. Mihaly Mezei for his assistance with computer support. We thank Dr. Diana Casper for reading the manuscript and offering helpful suggestions. This work is dedicated to and in memory of Dr. Lester A. Rubenstein, 2/9/1939–2/23/2004.

References

[1] R.A. Bond, P. Leff, T.D. Jonhson, C.A. Milano, H.A. Rockman, T.R. McMinn, S. Apparsundaram, M.F. Hyek, T.P. Kenakin, L.F. Allen, R.J. Lefkowitz, Physiological effects of inverse agonists in transgenic mice with myocardial overexpression of the beta-2-adrenoceptor, Nature 374 (1995) 272–276.

[2] T. Kenakin, Drug efficacy at G protein-coupled receptors, Annu. Rev. Pharmacol. Toxicol. 42 (2002) 349–379.

[3] R. Vogel, F. Siebert, Conformations of the active and inactive states of opsin, J. Biol. Chem. 276 (2001) 38487–38493.

[4] R.J. Lefkowitz, S. Cotecchia, P. Samama, T. Costa, Constitutive activity of receptors coupled to guanine nucleotide regulatory proteins, Trends Pharmacol. Sci. 14 (1993) 303–307.

[5] D. Colquhoun, Binding, gating, affinity and efficacy: the interpretation of structure–activity relationships for agonists and of the effects of mutating receptors, Br. J. Pharm. 125 (1998) 923–947.

[6] R. Lanzara, Method for Determining Drug Compositions to Prevent Desensitization of Cellular Receptors, U.S. Patent #5,597,699, 1997.

[7] R. Lanzara, Compositions to Enhance the Efficacy and Safety of Biopharmaceutical Drugs. U.S. Patent #6,593,094, 2003.

[8] R. Lanzara, Optimal agonist/antagonist combinations maintain receptor response by preventing rapid β_1-adrenergic receptor desensitization, Int. J. Pharm. 1 (2) (2005) 122–131.

[9] U.M. Ganter, T. Charitopoulos, N. Virmaux, F. Siebert, Conformational changes of cytosolic loops of bovine rhodopsin Fourier transform infrared difference spectroscopy, Photochem. Photobiol. 56 (1992) 57–62.

[10] T. Sakamoto, H.G. Khorana, Structure and function in rhodopsin: the fate of opsin formed upon the decay of light-activated metarhodopsin II in vitro, Proc. Natl. Acad. Sci. U.S.A. 92 (1995) 249–253.

[11] G.-F. Jang, V. Kuksa, S. Filipek, F. Bartli, E. Ritteri, M.H. Gelb, K.P. Hofmanni, K. Palczewski, Mechanism of rhodopsin activation as examined with ring-constrained retinal analogs and the crystal structure of the ground state protein, J. Biol. Chem. 276 (2001) 26148–26153.

[12] U. Gether, S. Lin, B.K. Kobilka, Fluorescent labeling of purified β-2 adrenergic receptor: evidence for ligand-specific conformational changes, J. Biol. Chem. 47 (1995) 28268–28275.

[13] J.A. Ballesteros, A.D. Jensen, G. Liapakis, S.G. Rasmussen, L. Shi, U. Gether, J.A. Javitch, Activation of the β2-adrenergic receptor involves disruption of an ionic lock between the cytoplasmic ends of transmembrane segments 3 and 6, J. Biol. Chem. 276 (2001) 29171–29177.

[14] S.G. Rasmussen, A.D. Jensen, G. Liapakis, P. Ghanouni, J.A. Javitch, U. Gether, Mutation of a highly conserved aspartic acid in the beta2 adrenergic receptor: constitutive activation, structural instability, and conformational rearrangement of transmembrane segment 6, Mol. Pharmacol. 56 (1999) 175–184.

[15] T.P. Sakmar, S.T. Menon, E.P. Marin, E.S. Awad, Rhodopsin: insights from recent structural studies, Annu. Rev. Biophys. Biomol. Struct. 31 (2002) 443–484.

[16] L. Rubenstein, R. Lanzara, Activation of G Protein-coupled receptors entails cysteine modulation of agonist binding, J. Mol. Struct. (THEOCHEM) 430 (1998) 57–71.

[17] P.C. Jocelyn, Biochemistry of the SH Group, Academic Press, New York, 1972.

[18] U. Gether, S. Lin, P. Ghanouni, J.A. Ballesteros, H. Weinstein, B.K. Kobilka, Agonists induce conformational changes in transmembrane domains III and VI of the β2 adrenoceptor, EMBO J. 16 (1997) 6737–6747.

[19] C.D. Strader, T.M. Fong, M.R. Tota, D. Underwood, R.A.F. Dixon, Structure and function of G protein-coupled receptors, Ann. Rev. Biochem. 63 (1994) 101–132.

[20] J.M. Baldwin, G.F.X. Schertler, V.M. Unger, An alpha carbon template for the transmembrane helices in the rhodopsin family of G-protein-coupled receptors, J. Mol. Biol. 272 (1997) 144–164.

[21] U. Gether, Uncovering molecular mechanisms involved in activation of G-protein-coupled receptors, Endocr. Rev. 21 (2000) 90–113.

[22] K. Palczemski, T. Kumasaka, T. Hori, C.A. Behnke, H. Motoshima, B.A. Fox, I. Le Trong, D.C. Teller, T. Okada, R.E. Stenkamp, M. Yamamoto, M. Miyano, Crystal structure of rhodopsin: a G protein-coupled receptor, Science 289 (2000) 739–745.

[23] J. Saranak, K.W. Foster, Reducing agents and light break an S–S bond activating rhodopsin in Vivo, Biochem. Biophys. Res. Commun. 275 (2000) 286–291.

[24] S.E. Pedersen, E.M. Ross, Functional activation of β-adrenergic receptors by thiols in the presence or absence of agonists, J. Biol. Chem. 260 (1985) 14150–14157.

[25] V.A. Florio, P.C. Sternweis, Mechanisms of muscarinic receptor action on Go in reconstituted phospholipid vesicles, J. Biol. Chem. 264 (1989) 3909–3915.

[26] A. Sidhu, A novel affinity purification of D-1 dopamine receptors from rat striatum, J. Biol. Chem. 265 (1990) 10065–10072.

[27] K. Kanematsu, R. Naito, Y. Shimohigashi, M. Ohno, T. Ogasawara, M. Kurono, K. Yagi, Design synthesis of an opioid receptor probe: mode of binding of S-Activated (−)-6β-sulfhydryldihydromorphine with the sh group in the μ-opioid receptor, Chem. Pharm. Bull. 38 (1990) 1438–1440.

[28] T.L. Gioannini, I. Onoprishvili, J.M. Hiller, E.J. Simon, Inactivation of the purified bovine μ opioid receptor by sulfhydryl reagents, Neurochem. Res. 24 (1999) 37–42.

[29] N. Shirasu, T. Kuromizu, H. Nakao, Y. Chuman, T. Nose, T. Costa, Y. Shimohigashi, Exploration of universal cysteines in the binding sites of three opioid receptor subtypes by disulfide-bonding affinity labeling with chemically activated thiol-containing dynorphin A analogs, J. Biochem. 126 (1999) 254–259.

[30] P. Heinonen, K. Koskua, M. Pihlavisto, A. Marjamäki, V. Cockcroft, J.-M. Savola, M. Scheinin, H. Lönnberg, A series of 6-(ω-methanesufonylthioalkoxy)-2-*N*-methyl-1,2,3,4-tetrahydroisoquinolines: cysteine-reactive molecular yardsticks for probing α_2-adrenergic receptors, Bioconj. Chem. 9 (1998) 358–364.

[31] W.L. Strauss, J.C. Venter, A sulfhydryl group of the canine cardiac beta-adrenergic receptor observed in the absence of hormone, Life Sci. 36 (1985) 1699–1706.

[32] R.A. Cerione, J. Codina, J.L. Benovic, R.J. Lefkowitz, L. Birnbaumer, M.G. Caron, The mammalian β2-adrenergic receptor: reconstitution of functional interactions between pure receptor and pure stimulatory nucleotide binding protein of the adenylate cyclase system, Biochemistry 23 (1984) 4519–4525.

[33] R.A. Cerione, J.W. Regan, H. Nakata, J. Codina, J.L. Benovic, P. Gierschik, R.L. Somers, A.M. Spiegel, L. Birnbaumer, R.J. Lefkowitz, M.G. Caron, Functional reconstitution of the α_2-adrenergic receptor with guanine nucleotide regulatory proteins in phospholipid vesicles, J. Biol. Chem. 261 (1986) 3901–3909.

[34] J. Fontaine, J.-P. Famaey, J. Reuse, Potentiation by sulphydryl agents of the responses of guinea-pig isolated ileum to various agonists, J. Pharm. Pharmacol. 36 (1984) 450–453.

[35] C.K. Mathews, K.E. Van Holde, Biochemistry, second ed., Benjamin/Cummings, New York, 1996, pp. 135–136.

[36] J. March, Advanced Organic Chemistry, McGraw-Hill, New York, 1968, p. 889.

[37] J.D. Helmann, Science's STKE, 2002, http://www.stke.org/cgi/content/full/sigtrans;2002/157/pe46.

[38] N.M. Giles, A.B. Watts, G.I. Giles, F.H. Fry, J.A. Littlechild, C. Jacob, Metal and redox modulation of cysteine protein function, Chem. Biol. 8 (2003) 677–693.

[39] A. Claiborne, T.C. Mallett, J.I. Yeh, J. Luba, D. Parsonage, Structural, redox, and mechanistic parameters for cysteine–sulfenic acid function in catalysis and regulation, Adv. Protein Chem. 58 (2001) 215–276.

[40] A. Scheer, F. Fanelli, T. Costa, P.G. De Benedetti, S. Cottechia, The activation process of the α_{1B}-adrenergic receptor: potential role of protonation and hydrophobicity of a highly conserved aspartate, Proc. Natl. Acad. Sci. U.S.A. 94 (1997) 808–813.

[41] A. Christopoulos, T. Kenakin, G protein-coupled receptor allosterism and complexing, Pharmacol. Rev. 54 (2002) 323–374.

[42] L. Oliviera, A.C.M. Paiva, C. Sander, G. Vriend, A common step for signal transduction in G protein-coupled receptors, Trends Pharmacol. Sci. 15 (1994) 170–172.

[43] G. Peleg, P. Ghanouni, B.K. Kobilka, R.N. Zare, Single-molecule spectroscopy of the β2 adrenergic receptor: observation of conformational substates in a membrane protein, Proc. Natl. Acad. Sci. U.S.A. 98 (2001) 8469–8474.

[44] Z.-L. Lu, J.W. Saldanha, E.C. Hulme, Transmembrane domains 4 and 7 of the M1 muscarinic acetylcholine receptor are critical for ligand binding and the receptor activation switch, J. Biol. Chem. 276 (2001) 34098–34104.

[45] P. Ghanouni, H. Schambye, R. Seifert, T.W. Lee, S.G. Rasmussen, U. Gether, B.K. Kobilka, The effect of pH on beta(2) adrenoceptor function: evidence for protonation-dependent activation, J. Biol. Chem. 275 (2000) 3121–3127.

[46] B.A. McSwiney, W.H. Newton, Reaction of smooth muscle to the H-ion concentration, J. Physiol. 63 (1927) 51–60.

[47] F.-Y. Zeng, J. Wess, Identification molecular characterization of M3 muscarinic receptor dimers, J. Biol. Chem. 274 (1999) 19487–19497.

[48] T.E. Hebert, S. Moffett, J.-P. Morello, T.P. Loisel, D.G. Bicheti, C. Barret, M. Bouvier, A peptide derived from a β2-adrenergic receptor transmembrane domain inhibits both receptor dimerization and activation, J. Biol. Chem. 271 (1996) 16384–16392.

[49] W. Guo, L. Shi, J.A. Javitch, The fourth transmembrane segment forms the interface of the dopamine D2 receptor homodimer, J. Biol. Chem. 278 (2003) 4385–4388.

[50] T. Kenakin, Efficacy at G-protein-coupled receptors, Nat. Rev. Drug Discov. 1 (2002) 103–110.

[51] N. Guex, M.C. Peitsch, SWISS-MODEL and the Swiss-PdbViewer: an environment for comparative protein modeling, Electrophoresis 18 (1997) 2714–2723. http://www.expasy.org/spdbv/.

[52] J.A. Ballesteros, H. Weinstein, Methods Neurosci. 25 (1995) 366–428.